Complex systems with half-integer spins: Symplectic ensembles

Rina Dutta and Pragya Shukla
Department of Physics, Indian Institute of Technology, Kharagpur, India
(Received 18 July 2007; published 28 November 2007)

We study the statistical behavior of the Hermitian operators of complex systems with half-integer angular momentum and time-reversal symmetry. The complexity leads to randomization of the operators which can then be modeled, following maximum entropy hypothesis, by multiparametric Gaussian ensembles of real-quaternion matrices. The modeling shows that it is possible to classify the statistical behavior of spin-based complex systems into a continuum of universality classes characterized by a single parameter which is a function of all system parameters.

DOI: 10.1103/PhysRevE.76.051124 PACS number(s): 05.40.−a, 05.30.−d, 05.45.−a, 89.75.−k

I. INTRODUCTION

Recent advances in science and technology have refocused our attention on the particle spin. For example, spintronics ("spin-based electronics") is an emergent technology which specifically exploits the spin properties of electron (and more generally nuclear) instead of or in addition to the charge degrees of freedom. The spin relaxation and spin transport in metals and semiconductors are of fundamental research interest not only for being basic solid state physics issues, but also for the already demonstrated potential these phenomena have in electronic technology [1–6]. In the domain of nanosystems, e.g., almost closed quantum dots, the spin-orbit coupling or spin-spin interaction can significantly influence the physical properties, e.g., transport and thermodynamics behavior [1,7]. As a consequence, it is imperative to seek more information about the role played by particle spin. The information promises a wide variety of new devices that combine logic, storage, and sensor applications and might lead to quantum computers and quantum communication based on electronic solid-state devices [2,5].

Fundamental interest in spin-physics stems from the requirement, posed by modern technologies, to control and probe systems on length scales larger than atoms but small enough to render averaging inapplicable. In a nanosystem, for example, the statistical average over many subsystems is not valid and the physical properties (e.g., conductance through the system) become sample dependent. For a massive production of any device, however, it is important to control the reproducibility of its physical properties. As a consequence, knowledge of the sample-to-sample fluctuations of the physical properties is important.

The physical properties of a system can in principle be formulated in terms of the eigenvalues and eigenfunctions of an operator associated with the system. The information about the fluctuation of the properties can then be derived from the distributions of the eigenvalues and eigenfunctions. This motivates us to pursue the present study where our focus is on the study of the distributions and their evolutions under varying system conditions for the conservative complex systems with half-integer spin. A similar analysis for the systems with integer spin is discussed in [8]. However, due to the quaternion nature of the matrices resulting from Kramers degeneracy, intermediate steps involved with derivation of the evolution equations for the half-integer cases are technically quite difficult which makes it necessary to study them separately. The first step in this direction is to describe the operator, e.g., Hamiltonian.

The conservative nature of the dynamics system requires its Hamiltonian to be Hermitian: $H^{\dagger}=H$. The presence of time-reversal symmetry along with half-integer total angular momentum in the system (that is $[H,T]=0$ with $T^2=-1$ where T is the time-reversal operator) leads to Kramers degeneracy (double degeneracy of the eigenvalues) too [9]. As a consequence, the Hamiltonian matrix can be most suitably represented by a basis consisting of states, say ϕ_k and their time-reversed pairs $T\phi_k$, $k=1\rightarrow N$. The latter allows the matrix to be expressed in a quaternion form, $H_{kl}\equiv\Sigma_{s=1}^{4}H_{kl;s}\tau_s$ with $k,l=1\rightarrow N$, $\tau_1=I$, and $\tau_s=i\sigma_{s-1}$ where $s=2,3,4$ and σ_{s-1} as the three Pauli matrices [9].

Under Kramers degeneracy, T can be expressed in a simple form, $T=\tau_2 K$ with K as the complex conjugation operator [9]. The time-reversal symmetry ($H=THT^{-1}$) now implies

$$H_{kl}=-\tau_2 H_{kl}^{*}\tau_2=-\tau_2\left(\sum_{s=1}^{4}H_{kl;s}^{*}\tau_s^{*}\right)\tau_2=\sum_{s=1}^{4}H_{kl;s}^{*}\tau_s. \quad (1)$$

The time-reversal symmetry therefore reduces H to be a quaternion real matrix, $H_{kl;s}=H_{kl;s}^{*}$ (for all k, l, s). The Hermiticity of H ($H_{kl}=H_{kl}^{\dagger}$) further leads to $H_{kl;s}=a_s H_{lk;s}$ with $a_1=1$ and $a_2=a_3=a_4=-1$. The Hamiltonian of a time-reversal conservative system with half-integer angular momentum can then be written as a $N\times N$ Hermitian matrix with real-quaternion elements, $H_{kl}\equiv\Sigma_{s=1}^{4}H_{kl;s}\tau_s=\Sigma_{s=1}^{4}a_s H_{lk;s}\tau_s$ with $k,l=1\rightarrow N$ and $H_{kl;s}$ as real numbers [9]. (Note each H_{kl} is a 2×2 matrix but $H_{kl;s}$ are just numbers.)

Besides symmetry requirements, the structure of the matrix representing the operator also depends on the nature of the complexity in the system. The complexity may have its origin in the complicated interactions among various subunits of a many-body system, e.g., nuclei, atoms, molecules, etc., or due to complicated interference of high-lying eigenstates of a simple system, e.g., quantum chaotic system. It may also originate due to scattering from impurities, e.g., a disordered system or from boundaries of the confining geometry of a clean system, e.g., a quantum dot. The ultimate effect of various sources of complexity in general is to render

exact determination of the matrix element, say $H_{kl} \equiv \langle k|H|l\rangle$ with $|k\rangle$, $|l\rangle$ as the basis vectors in a physically relevant basis, technically difficult. As a consequence, each matrix element can be best described by a distribution with its moments, e.g., variance, mean reflecting the nature of physical constraints, e.g., localized or delocalized wave dynamics, interactions, scattering and boundary conditions, dimensionality, etc.

A prior knowledge of the joint probability density of all the matrix elements, termed also as ensemble density, is necessary to determine the distributions of the eigenvalues and eigenfunctions. In this paper, we consider a multiparametric Gaussian ensemble density which can model a wide range of complex systems; this is explained by an example described in the next section. In principle, an integration of the ensemble density over undesirable variables, e.g., eigenvectors or eigenvalues will give the distributions of eigenvalues or eigenvectors, respectively. However, this route being technically difficult, we choose to explore the diffusion route described in Sec. III. The diffusion equation of the ensemble density is then used in Sec. IV to formulate the diffusion of the eigenvalues and eigenfunctions; as described in Sec. V, the implications of the formulation are numerically verified. The analytical results well supported by our numerical analysis lead to concluding remarks given in Sec. VI.

II. SYSTEMS WITH REAL-QUATERNION MATRIX REPRESENTATION: AN EXAMPLE

The examples of such systems appear in many branches of physics, e.g., nuclear physics [10,11], condensed matter physics [1,2,5,7,12], quantum chaos [13], etc. As an example, let us consider the case of an Anderson system, a d-dimensional disordered system of fermions (with spin-1/2) with spin-orbit coupling (SOC) [12]. Within tight-binding approximation, the Hamiltonian H of the system can be described as

$$H = \sum_{n,\sigma} \epsilon_n |n,\sigma\rangle\langle n,\sigma| + \sum_{n\neq m,\sigma,\sigma'} V_{nm}^{\sigma\sigma'} |n,\sigma\rangle\langle m,\sigma'|. \quad (2)$$

Here $\sigma = \pm 1/2$ and n refers to the lattice sites, $n = 1 \to L^d$, ϵ_n is the spin-independent, on-site random potential. The hopping is assumed to connect only the z nearest neighbors (referred to by m) of each site. In the site basis, each matrix element of H is a 2×2 matrix (due to two component spinor space associated with each site), $H_{kl} = \begin{pmatrix} H_{kl}^{\sigma\sigma} & H_{kl}^{\sigma\sigma'} \\ H_{kl}^{\sigma'\sigma} & H_{kl}^{\sigma'\sigma'} \end{pmatrix}$ with $H_{kl}^{\sigma\sigma'} = \langle k\sigma|H|l\sigma'\rangle$. Thus, H can be written as a real-quaternion sparse matrix of size $N = L^d$ with diagonal matrix elements as the site energies $H_{kk} = \epsilon_k \tau_1$. The off-diagonal H_{kl}, describing the hopping interaction between two sites k and l, are 2×2 matrices describing spin rotation due to the SOC on every lattice bond (k,l),

$$H_{kl} = V_{kl;1}\tau_1 + \mu \sum_{s=2}^{4} V_{kl;s}\tau_s \equiv \begin{bmatrix} V_{kl;1} + i\mu V_{kl;4} & \mu(V_{kl;3} + iV_{kl;2}) \\ -\mu(V_{kl;3} + iV_{kl;2}) & V_{kl;1} - i\mu V_{kl;4} \end{bmatrix}, \quad (3)$$

where μ denotes the SOC coupling and $V_{kl;s}$ are real and independent random variables; for simplification we take $V_{kl;1} = 1$.

The randomness of the on-site potential ϵ_k and hopping terms V_{kl} permits a possible description of $H_{kk} = H_{kk;1} = \epsilon_k \tau_1$, $H_{kl;1} = \tau_1$, and $H_{kl;s} = \mu V_{kl;s}\tau_s$ (for $s = 2,3,4$ and $k \neq l$) only by the distributions, say, $\rho_{kk}(H_{kk})$ and $\rho_{kl}(H_{kl})$, respectively. Let us consider the isotropic case when ϵ_k and $V_{kl;s}$ are Gaussian distributed with zero mean and variances ω and η, respectively. This gives $\rho_{kk}(H_{kk}) = e^{-H_{kk}^2/2\omega}$, $\rho_{kl;1}(H_{kl;1}) = \delta(H_{kl;1} - 1)$, $\rho_{kl;s}(H_{kl;s}) = e^{-H_{kl;s}^2/2\mu^2\eta}$ (with $s = 2 \to 4$) for each (k,l) pair connected by hopping; here the variances ω and η depend on the system conditions, e.g., disorder and spin-orbit interactions. The lack of hopping between two sites, say k', l', gives $H_{k'l'} = 0$ which implies $\rho_{k'l'}(H_{k'l'}) = \delta(H_{k'l'})$. The probability density $\rho(H) \equiv \Pi_{k,l;k\leq l}\rho_{kl;s}(H_{kl;s})$ of the Anderson ensemble (AE) can then be given by

$$\rho(H,v,b) = C \exp\left(-\sum_k H_{kk}^2/2\omega - \sum_{s=2}^{4} \sum_{(k,l)=n.n.} H_{kl;s}^2/2\mu^2\eta \right) \times \prod_{(k,l)=n.n} \delta(H_{kl;1} - 1) \prod_{(k,l)\neq n.n.} \delta(H_{kl}) \quad (4)$$

with C as the normalization constant. Note, for later reference, that the δ-function terms above can also be written as the limiting Gaussians $[\delta(x) = \lim_{v\to 0}(2\pi v^2)^{-1/2} e^{-x^2/2v^2}]$.

The above example corresponds to a specific case of a spin system with on-site disorder and isotropic nearest-neighbor random hopping. In general, the hopping can also be long-range and/or anisotropic, nonrandom or random with a nonrandom component. To describe all such possibilities, we consider an ensemble of $2N\times 2N$ Hermitian matrices H with real-quaternion elements H_{kl} distributed as Gaussians with arbitrary mean and variances; the four linearly independent components of each matrix element are chosen to be statistically independent. A general form of the probability density $\rho(H) \equiv \Pi_{k,l;k\leq l}\rho_{kl}(H_{kl})$ of the ensemble can then be given by

$$\rho(H,h,b) = C \exp\left(-\sum_{s=1}^{4} \sum_{k\leq l} (1/2v_{kl;s})(H_{kl;s} - b_{kl;s})^2 \right) \quad (5)$$

with subscript "s" of a variable referring to its components, v as the matrix of the variances $v_{kl;s} = \langle H_{kl;s}^2\rangle - \langle H_{kl;s}\rangle^2$, and b as the matrix of all mean values $\langle H_{kl;s}\rangle = b_{kl;s}$. As obvious, in the limit $v_{kl;s} \to 0$, Eq. (5) contains a nonrandom contribution from $H_{kl;s}$ [as $\rho_{kl}(H_{kl;s}) \to \delta(H_{kl;s} - b_{kl;s})$]. Note Eq. (4) is a special case of Eq. (5) with

$$v_{kk} = \omega, \quad b_{kk} = 0,$$

$$v_{kl;s} = \eta\mu^2(1 - \delta_{s1})f_{kl}, \quad b_{kl;s} = \delta_{s1}f_{kl}, \quad (6)$$

where $f_{kl} = 1$ for the connected $\{k,l\}$ pairs, and $f_{kl} = 0$ for all $\{k,l\}$ indices corresponding to disconnected pairs of sites. Equation (5) can also model the cases with hopping to be anisotropic (by choosing different variances for connected pairs), nonrandom or random (by choosing zero or nonzero variances for connected pairs). Further, note that Eq. (5)

gives the Gaussian symplectic ensemble (GSE) in the limit $2v_{kl;s}=v_{kk}=\gamma^{-1}$, $b_{kl;s}=0$, $\rho \propto e^{-(\gamma/2)\mathrm{Tr}\, H^2}$.

In the example described by Eq. (4), the randomness of the matrix elements is caused due to impurities. As mentioned above, the presence of other types of complicated interactions can also make the exact determination of the matrix elements difficult. The elements are then best described by a distribution which can be determined by the maximum entropy principle (MEP) subjected to known physical constraints [14]. For example, MEP predicts a Gaussian distribution of a variable if its average behavior and variance are the only known constraints. As a consequence, the half-integer spin systems with randomness originated from sources other than disorder can also be modeled by the ensemble density (5).

III. SINGLE PARAMETRIC EVOLUTION OF THE MULTIPARAMETRIC ENSEMBLE DENSITY

The distribution parameters of ρ are basically a measure of the degree of inexactness associated with the determination of the matrix elements due to existing system conditions. A change of the latter may therefore affect the distribution parameters of ρ and thereby its statistical properties. Using Gaussian nature of ρ, it is easy to verify that under a change of the parameters $v_{kl;s} \to v_{kl;s}+\delta v_{kl;s}$ and $b_{kl;s} \to b_{kl;s}+\delta b_{kl;s}$, the matrix elements H_{kl} undergo a diffusion dynamics along with a finite drift,

$$T\rho = L\rho, \tag{7}$$

where

$$T \equiv \sum_{j=1}^{M} \frac{\partial}{\partial f_j},$$

$$L \equiv \sum_{kl;s} \frac{\partial}{\partial H_{kl;s}} \left(\frac{g_{kl}}{2} \frac{\partial}{\partial H_{kl;s}} + \gamma H_{kl;s} \right) \tag{8}$$

with

$$f_j = (1/2)\ln|x_{kl;s}| + c_j \quad \text{for } j = 1 \to M_1,$$

$$f_j = \ln|b_{kl;s}| + C_j \quad \text{for } j > M_1. \tag{9}$$

Here $x_{kl;s} \equiv 1-\gamma \tilde{g}_{kl} v_{kl;s}$ with $\tilde{g}_{kl}=2-\delta_{kl}$ and $g_{kl}=1+\delta_{kl}$, with M_1 and $M-M_1$ as the number of nonzero parameters $x_{kl;s}$ and $b_{kl;s}$, respectively. The parameter γ is arbitrary, giving the variance of the matrix elements at the end of the evolution [8].

Equation (7) describes a multiparametric flow of matrix elements from an arbitrary initial condition, say H_0. It is possible, however, to define a single parameter Y which satisfies the condition $T\rho=\partial_Y \rho$. Thus, matrix elements undergo a single parametric diffusion with respect to Y,

$$\frac{\partial \rho}{\partial Y} = L\rho. \tag{10}$$

The parameter Y can be obtained by solving the condition $T=\partial_Y$; the existence of a solution requires the following condition to be fulfilled:

$$\alpha_n A_m^2 \partial_{f_m} A_n = \alpha_m A_n^2 \partial_{f_n} A_m, \tag{11}$$

where α are arbitrary constants and $A_j=\alpha_j(\partial_{f_j} Y)^{-1} \times (\Sigma_{k=1}^{N} \alpha_k)^{-1}$ [15]. Choosing $\alpha_j=1$ (for all j) with f_j given by Eq. (9), it is easy to show that the above condition is fulfilled and Y can be given as

$$Y = -\frac{1}{2M\gamma} \ln\left(\prod_{k\le l}{}' \prod_{s=1}^{4} |x_{kl;s}||b_{kl;s}|^2 \right) + C, \tag{12}$$

here Π' implies a product over nonzero parameters $b_{kl;s}$ and $x_{kl;s}$ with M as their total number. Further, C is a constant determined by the initial distribution. Being a function of various distribution parameters $v_{kl;s}$ and $b_{kl;s}$, Y can be referred to as the complexity parameter. (Note, as for the real-symmetric and complex Hermitian cases, Y can also be derived by alternative methods, discussed in [8,16].) As examples, here we consider Y for three specific cases of the real-quaternion matrices (also useful for later reference):

(i) *Ensemble of diagonal matrices.* This case can be described by the distribution parameter

$$\langle H_{kl;s}^2 \rangle = v_{kl;s} = (2\nu_k)^{-1} \delta_{kl}\delta_{s1}, \quad \langle H_{kl} \rangle = b_{kl} = 0. \tag{13}$$

A substitution of the above in Eq. (12) gives Y,

$$Y = -(2\gamma M)^{-1} \sum_k \ln|1-(\gamma/2\nu_k)| + \text{const}. \tag{14}$$

Note here, all $x_{kl;s}$ being nonzero, one has $M=N(2N-1)$.

(ii) *Case with constant ratio of the diagonal and off-diagonal variances.* Consider the case described by the distribution

$$\langle H_{kl;s}^2 \rangle = v_{kl;s} = (4\gamma)^{-1}[2\delta_{kl} + (1-\delta_{kl})(1+\mu)^{-1}],$$

$$\langle H_{kl} \rangle = b_{kl} = 0; \tag{15}$$

the complexity parameter Y corresponding to this case is [with $M=N(2N-1)$]

$$Y = -N(2\gamma M)^{-1}\{2(N-1)\ln|1-[4(1+\mu)]^{-1}| - \ln 2\} + \text{const}. \tag{16}$$

Note this case can also describe an ensemble of Anderson Hamiltonians with very long range, isotropic, random hopping. Also note that the limit $\mu \to 0$ corresponds to the Gaussian symplectic ensemble case [9] [as $\langle H_{kk}^2 \rangle = 2\langle H_{kl;s}^2 \rangle$ from Eq. (15)]. Similarly the limit $\mu \to \infty$ (corresponding to diagonal ensembles) gives Y the same as in Eq. (14) with $\nu_k=\gamma$.

(iii) *Anderson ensemble.* The substitution of parameters given by Eq. (6) in Eq. (12) gives Y for the ensemble of the Hamiltonians (2),

$$Y = -\frac{N}{2M\gamma}\alpha + \text{const} \tag{17}$$

with $\alpha=\ln|1-\gamma\omega|+(3z/2)\ln[|1-2\gamma\mu^2\eta|]$. Here $M=N(4N+z-2)/2$ [due to $N+2N(N-1)$ nonzero contributions from

$x_{kl;s}$, where $k,l=1,\ldots,N$ (with $k\geq l$), and $zN/2$ nonzero contributions from $b_{mn;1}$ values for nearest-neighbor pairs H_{mn}].

The solution of Eq. (10) gives the state $\rho(H,Y|H_0,Y_0)$ of the flow at parameter Y, starting from an arbitrary initial state H_0 with $Y=Y_0$. An integration over initial probability density results in the Y governed density, $\rho(H,Y)=\int\rho(H,Y|H_0,Y_0)\rho(H_0,Y_0)dH_0$. The evolution reaches a steady state when $\partial\rho/\partial Y\to 0$ (equivalently $\tilde{g}_{kl}v_{kl;s}\to\gamma^{-1}$, $b_{kl;s}\to 0$), with the solution $\rho(H)$ approaching the Gaussian symplectic ensemble [this is expected as the limit $\tilde{g}_{kl}v_{kl;s}\to\gamma^{-1}$, $b_{kl;s}\to 0$ of Eq. (4) corresponds to a GSE too].

IV. COMPLEXITY PARAMETER GOVERNED DIFFUSION OF THE EIGENVALUES AND THE EIGENFUNCTIONS

The eigenvalue equation of an $N\times N$ real-quaternion Hermitian matrix H is given by $HS=S\Lambda$ with Λ as the $N\times N$ real-quaternion matrix of eigenvalues, $\Lambda_{mn}=\lambda_n\tau_1\delta_{mn}$ and S as the $N\times N$ real-quaternion eigenvector matrix, symplectic in nature, $S^RS=S\tau_2S^T=\tau_2$ where $S^R=S^+=S^{-1}$ [9].

The joint probability density of the eigenvalues can be defined as follows: Let $P_E[\{E_n\},Y(v,b)]$ be the joint probability of finding eigenvalues λ_i of H between E_i and E_i+dE_i $(i=1,2,\ldots,N)$ for given v and b matrices, it can then be expressed as

$$P_E(\{E_n\},Y)=\int\prod_{i=1}^{N}\delta(E_i-\lambda_i)\rho(H,Y)dH. \tag{18}$$

The joint probability density P_{Nq} of the components S_{nk} $(n=1\to N)$ of q eigenvectors S_k $(k=1\to q)$ can similarly be defined as

$$P_{Nq}(Z_1,Z_2,\ldots,Z_q,Y)=\int\prod_{k=1}^{q}\tilde{f}_k\rho(H,Y)dH, \tag{19}$$

where $\tilde{f}_k=\delta(Z_k-S_k)\delta(Z_k^R-S_k^R)\delta(e_k-\lambda_k)$.

As mentioned above, the information about system conditions is contained in ρ and therefore P_E and P_{Nq} through Y. The effect of the variation of system conditions (e.g., disorder, boundary conditions, etc., in the samples) can therefore be determined by a knowledge of the Y-governed evolution of P_E or P_{Nq}. As for the ensembles of real symmetric matrices ($\beta=1$) and complex Hermitian matrices ($\beta=2$) [17], the latter can also be derived by first taking the Y derivatives of Eqs. (18) and (19) and subsequently using Eq. (10). Note that, although the form of Eq. (10) is the same as for the $\beta=1,2$ cases [16,17], it is not obvious, however, that the diffusion equations for the eigenvalues and eigenvectors of the symplectic case will also be analogous to the $\beta=1,2$ cases. This is because the derivation of the equations from Eq. (10) is based on the responses of the eigenvalues λ_n and eigenfunctions S_n to a slight perturbation of H_{kl}. Due to the quaternion form of H_{kl}, the responses for real-quaternion Hermitian matrices are different from those for the $\beta=1,2$ cases,

$$\frac{\partial\lambda_n}{\partial H_{kl;s}}=\frac{1}{g_{kl}}(S_{nk}^R\tau_sS_{ln}+a_sS_{nl}^R\tau_sS_{kn}), \tag{20}$$

$$\frac{\partial S_{rn}}{\partial H_{kl;s}}=\frac{1}{g_{kl}}\sum_{m\neq n}\frac{S_{rm}}{\lambda_n-\lambda_m}(S_{mk}^R\tau_sS_{ln}+a_sS_{ml}^R\tau_sS_{kn}), \tag{21}$$

$$\frac{\partial S_{nr}^R}{\partial H_{kl;s}}=\frac{1}{g_{kl}}\sum_{m\neq n}\frac{1}{\lambda_n-\lambda_m}(S_{nk}^R\tau_sS_{lm}+a_sS_{nl}^R\tau_sS_{km})S_{mr}^R, \tag{22}$$

where $g_{kl}=1+\delta_{kl}$ (see Appendix A for the proof). Note that, contrary to $\beta=1,2$ cases [8], the order of variables are important in the above equations, S_{kl} and τ being 2×2 matrices, which makes them technically more difficult to use for the derivations of the following equations (see Appendix B for details):

$$\sum_{s=1}^{4}\sum_{k\leq l}\frac{\partial\lambda_n}{\partial H_{kl;s}}H_{kl;s}=\lambda_n, \tag{23}$$

$$\sum_{s=1}^{4}\sum_{k\leq l}g_{kl}\frac{\partial\lambda_n}{\partial H_{kl;s}}\frac{\partial\lambda_m}{\partial H_{kl;s}}=2\delta_{mn}, \tag{24}$$

$$\sum_{s=1}^{4}\sum_{k\leq l}g_{kl}\frac{\partial^2\lambda_n}{\partial H_{kl;s}^2}=8\sum_{m}\frac{1}{\lambda_n-\lambda_m}. \tag{25}$$

The substitution of Eq. (10) in the Y derivative of P_E, followed by a partial integration and subsequent use of Eqs. (23)–(25), leads to the diffusion equation for the eigenvalues

$$\frac{\partial P_E}{\partial Y}=\sum_n\frac{\partial}{\partial E_n}\left(\frac{\partial}{\partial E_n}+\sum_{m\neq n}\frac{\beta}{E_m-E_n}+\gamma E_n\right)P_E, \tag{26}$$

where $\beta=4$. Note that the form of the above equation is similar to the $\beta=1,2$ cases (see [8]).

Equation (26) is analogous to the equation governing the evolution of eigenvalues of the Brownian ensembles (BE), consisting of real-quaternion matrices [9,18] [a similar analogy exists between $\beta=1,2$ variants of the ensemble (5) and corresponding BEs too, see [8]]. The particular class of Brownian ensemble can be described as a nonstationary state undergoing a crossover due to a perturbation of a Hermitian matrix H_0 by a real-quaternion random Hermitian matrix V taken from GSE (see [8,9,18,19] for the details on BEs), $H=\sqrt{f}(H_0+\lambda V)$ [with $f=(1-\lambda^2)^{-1}$]. In the diagonal representation of the initial state H_0, the random perturbation V (of strength Λ) belongs to GSE. Note that the ensemble density of the above class of BEs can also be represented by Eq. (5) with variances and mean of the matrix elements given by Eq. (15) with $(1+\mu)=(\lambda^2f)^{-1}$; Y for BE is then given by Eq. (16) too.

Similar to the P_E case, P_{Nq} for various transition stages can be obtained by first substituting Eq. (10) in the Y derivative of Eq. (19) and then simplifying it by partial integration. This, however, requires the following relations (besides those for the eigenvalues):

$$\sum_{k;l,s;k\leq l}\frac{\partial S_{nj}}{\partial H_{kl;s}}H_{kl;s}=0, \tag{27}$$

$$\sum_{k,l,s;k\le l} \frac{g_{kl}}{2} \frac{\partial^2 S_{nj}}{\partial H_{kl;s}^2} = -\sum_{m\neq j} \frac{S_{nj}}{(\lambda_j - \lambda_m)^2}, \tag{28}$$

$$\sum_{k,l,s;k\le l} g_{kl} \frac{\partial \lambda_i}{\partial H_{kl;s}} \frac{\partial S_{nj}}{\partial H_{kl;s}} = 0, \tag{29}$$

$$\sum_{k,l,s;k\le l} g_{kl} \frac{\partial S_{ni}}{\partial H_{kl;s}} \frac{\partial S_{pj}}{\partial H_{kl;s}} = -\beta \frac{S_{ni}S_{pj}}{(\lambda_i - \lambda_j)^2}(1-\delta_{ij}), \tag{30}$$

$$\sum_{k,l,s;k\le l} g_{kl} \frac{\partial S_{ni}}{\partial H_{kl;s}} \frac{\partial S_{pj}^R}{\partial H_{kl;s}} = \beta \sum_{m\neq j} \frac{S_{nm}S_{pm}^R}{(\lambda_j - \lambda_m)^2}\delta_{ij}. \tag{31}$$

The above equations can again be derived from Eqs. (20)–(22) following steps similar to those given in Appendix B for Eqs. (23)–(25).

The reduction of the integrals over matrix elements H_{kl}, appearing in the Y derivatives of P_{Nq}, to the derivatives with respect to the eigenfunction components is discussed in detail in [17] for $\beta=1,2$ cases. Following similar steps and with the help of Eqs. (27)–(31), we obtain

$$\frac{\partial P_{Nq}}{\partial Y} = \sum_{k=1}^{q} (\tilde{F}_k + \tilde{F}_k^R + L_{e_k} P_{Nq}), \tag{32}$$

where

$$\tilde{F}_k = F_k + 2\sum_{l=1;\neq k}^{q} \sum_{m,n=1}^{N} \frac{\partial^2}{\partial z_{nk}\, \partial z_{ml}} \left(\frac{z_{nk} z_{ml}}{(e_k - e_l)^2} \right) P_{Nq} \tag{33}$$

with

$$F_K = \frac{2}{D_{\text{local}}^2} \sum_{n=1}^{N} \frac{\partial}{\partial z_{nk}} \left(\sum_m \frac{\partial h_2}{\partial z_{mk}^R} + h_1 \right), \tag{34}$$

and $\tilde{F}_K^R$ is similar to $\tilde{F}_K$ with each component z_{ak} of the eigenvector Z_k replaced by z_{ak}^R. Here $h_1=\chi(N-1)P_{Nq}$, $h_2=\chi(\delta_{mn}-\Sigma_{l=1}^q z_{ml}^R z_{nl})P_{Nq}$ with $\chi\to 1$ for $\mu<\zeta_k^d$, $\chi\to\mu/\zeta_k^d$ for $\mu>\zeta_k^d$ where $\mu=(e^{-2\gamma(Y-Y_0)}-1)^{-1}$ and ζ_k is the localization length of the kth eigenvector.

The steady states of the above evolution are again given by the limit $\partial P_{Nq}/\partial Y\to 0$. As for P_E, the solution of Eq. (32) in this limit turns out to be the corresponding distributions of a Gaussian symplectic ensemble (see [9] for the latter). Note that the form of Eq. (32) is the same as for the $\beta=1,2$ cases [17] except now z_{nk} are 2×2 matrices and with the following replacements: $z_{nk}^*\to z_{nk}^R$ and $\beta^2/4\to 2$.

Equation (32) can further be used to derive the diffusion equations for various other combinations of the eigenfunction components; for example, the distribution P_{r1} (distribution of the r components of just one eigenstate, say j) is given by the integration of Eq. (32) over all components of $q-1$ eigenstates (except jth) and only the undesirable $N-r$ components of the jth eigenstate. The equations are important as they can lead to Y-dependent formulation of the ensemble average as well as the distribution of any measure of the eigenfunction correlations. (A knowledge of the distribution is required because the strength of the reproducible fluctuations of different realizations of a same complex system can be of the order of the averages.) The derivation of the Y governed distributions of the measures, starting from Eq. (32), is discussed in detail in [17] for $\beta=1,2$ cases. However, due to the quaternion form of the variables, the derivations for the $\beta=4$ case are technically more difficult and require a detailed discussion; we hope to present it in a separate paper in the near future.

Equations (26) and (32) show that the fluctuations of the eigenvalues and the eigenfunctions are governed by a single parameter Y. However, the need to compare fluctuations against the same background requires a rescaling of the eigenvalues and eigenfunctions and therefore Y [9,17]. The rescaling of Y is measure based, with rescaled complexity parameters given as

$$\Lambda_{\text{measure}} = c_{\text{measure}} |Y - Y_0| / D_{\text{local}}^2. \tag{35}$$

Here D_{local} refers to the local mean-level density and c_{measure} depends on the nature of the fluctuation measure under consideration; for example, $c_e=1$ for all eigenvalue fluctuations (except mean-level density), however, it can vary for eigenvector fluctuation measures. The reason for a measure based rescaling of the complexity parameter Y is discussed in some detail in [17] for real-symmetric and complex Hermitian cases; the analogous form of Eq. (32) (notwithstanding quaternion variables) suggests it to be valid for the symplectic case too. Thus, we believe that, analogous to $\beta=1,2$ cases, the parameters Λ_u, Λ_{ip} for the local intensity $u=|z_{nk}|^2$ and the inverse participation ratio $I_2=\Sigma_{n=1}^{2N}|z_{nk}|^4$, respectively, of an eigenfunction, say Z_k (see [17] for the definition of these measures) can be given as

$$\Lambda_u = \mu^{-1}\Lambda_e, \quad \Lambda_{ip} = 2\chi\Lambda_e, \tag{36}$$

where $\Lambda_e=(Y-Y_0)/D_{\text{local}}^2$ is the rescaled spectral complexity parameter and the parameters μ and χ are the same as in Eq. (34). [Note that Eq. (32) of [17] contains a misprint: Λ_u appearing in the equation should read as Λ. Further, the correct definition of Λ_u is given above in Eq. (36) (instead of $\Lambda_u=\mu\Lambda$ reported in [17]).]

Our analytical results indicate the same behavior of the spectral fluctuation measures of different complex systems [i.e., different v,b matrices in Eq. (5)] with half-integer spin if their complexity parameters Λ_e are equal. The statistical spectral behavior of all complex systems modeled by Eq. (5) can therefore be classified in different universality classes described by Λ_e. The possibility of a continuous variation of Λ_e indicates the existence of infinitely many such classes. The same classification can also be applied for the measures related to the eigenfunction correlations. Although the latter are governed by two parameters Λ_{measure} as well as the system size N, however, Λ_{measure} is related to Λ_e [17].

Another important application of the Λ formulation is to explore the possibility of a critical behavior of the system [17] which can briefly be explained as follows: Due to N dependence of Λ, the variation of the physical conditions in an infinite-size system in general leads to one of the two limits, either $\Lambda\to 0$ or $\Lambda\to\infty$. Contrary to finite-size behavior, the statistical behavior in the limit $N\to\infty$ therefore corresponds to only one of the two universality classes, namely,

the initial state ($\Lambda \to 0$) or the steady state, i.e., Gaussian symplectic ensemble ($\Lambda \to \infty$). A new universality class of the statistics, referred to as the critical statistics, however, may appear even in the infinite-size limit if the system parameters satisfy the condition $\lim_{N\to\infty} \Lambda(v,b,N) \to \Lambda_{\text{critical}}$ where $\Lambda_{\text{critical}}$ is nonzero and finite (the latter is an indicator of the statistical behavior different from those at $\Lambda = 0, \infty$ limits). For example, contrary to the spinless case, it is possible to find a critical disorder for the two-dimensional Anderson Hamiltonian with spin-orbit scattering which leads to nonzero, finite Λ, even in the infinite-size limit. This is because the spin-orbit interaction leads to an enhancement of the localization length ζ [12] and which may result in a finite, nonzero Λ, even in the infinite-size limit. (For the $d=2$ spinless cases, ζ being an exponential function of the mean free path only, $\Lambda \to 0$ in the limit $N \to \infty$ [20]. This explains the observed lack of critical point for $d=2$ spinless cases.)

As mentioned above, a BE is a specific case of Eq. (5) with distribution parameters given by Eq. (15) and Y given by Eq. (16). The diffusion equations (26) and (32) for the ensemble (5) are therefore applicable for the BEs too, appearing during the initial ensemble → Gaussian symplectic ensemble transition. This further implies the analogy of various fluctuation measures for the two cases if their rescaled complexity parameters are the same (and system size is also the same for the eigenfunction measures) [17]. The analogy can be utilized to a great advantage. The single parametric BEs are technically easily tractable as compared to Eq. (5) and many of their statistical spectral properties are already known [19]. The information about the symplectic class of BEs can then be used to derive the statistical properties of many complex systems with half-integer spin represented by ensemble (5).

V. NUMERICAL ANALYSIS

To reconfirm the statistical analogy of the systems represented by Eq. (5) with BEs, we numerically compare the fluctuation measures of a prototype complex system, namely, the AE with those of BEs.

(i) *Anderson ensemble.* For numerical analysis, we consider a square Anderson lattice of linear size L ($N=L^2$) with its Hamiltonian described by Eq. (2). The spin-independent on-site potential ϵ_k is a random variable chosen from a Gaussian distribution of variance $\omega = W^2/12$, $W=2.92$ and mean zero. The hopping is chosen to be between nearest neighbors, isotropic and random; the hopping matrix element H_{kl} is described by Eq. (3) with SOC coupling strength $\mu = 2$ and variables $V_{kl;s}$ ($s=2,3,4$) as random variables chosen from a Gaussian distribution with mean zero and variance $\eta = V_1/12$, where $V_1 = 0.5$ [12]. (As indicated by our numerics, the chosen parameter values correspond to the critical regime. Note that, for the case with uniform distributed on-site potential, the critical point is found to occur at disorder values $W=8.55$, $V_1=1$ [12].) A substitution of the above values in Eq. (17) gives $Y \approx -\alpha/4N$ with $\alpha = 3.68$ (for the choice of $\gamma = 1$).

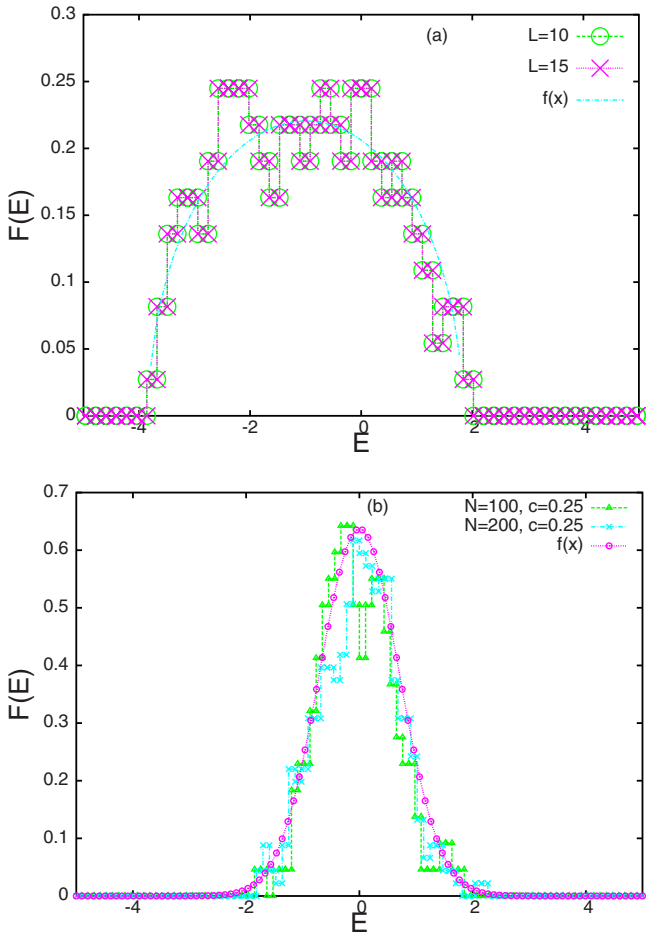

FIG. 1. (Color online) The behavior of level density $F(E) = (ND)^{-1}$: (a) for the AE for two system sizes $L=10$ and $L=15$. The numerical fitted function $f(x)$ (with $x=E$) has the form $F(E) = \sqrt{9-(E+0.5)^2}/\pi$; (b) for the critical BE analog ($c=0.25$) of the higher-order spectral correlations of the AE considered in (a). Here F is well fitted by the function $F(E) = f_1 e^{-E^2}$ with $f_1 = 2/\pi$. Note the lack of analogy between the mean-level densities for the cases given in (a) and (b) while their higher-order spectral correlations (shown in Fig. 4) are approximately the same. This is consistent with the theory (see [8,19]). The numerical analysis of F for the BE cases $c=0.03$ and $c=0.4$ gives $f_1 = \pi^{-1/2}$ and $2/\pi$, respectively; as shown in Figs. 6 and 7, these BEs are the analogs for the eigenfunction measures, namely, local eigenfunction intensity and inverse participation ratio.

The calculation of Λ requires the choice of a physically suitable initial state H_0. We choose H_0 as an insulator, represented by an ensemble of diagonal matrices with distribution parameters given by Eq. (13) (taking $\nu_{kk} = \gamma$ for all k); the statistics of the eigenvalues for H_0 corresponds to the Poisson distribution and with completely localized eigenfunctions. Following Eq. (14), the complexity parameter for the initial state can then be given as $Y_0 = -\alpha_0/4N$ with $\alpha_0 = \ln 2$.

Using Y and Y_0 in Eq. (35), the spectral complexity parameter Λ_e can be obtained,

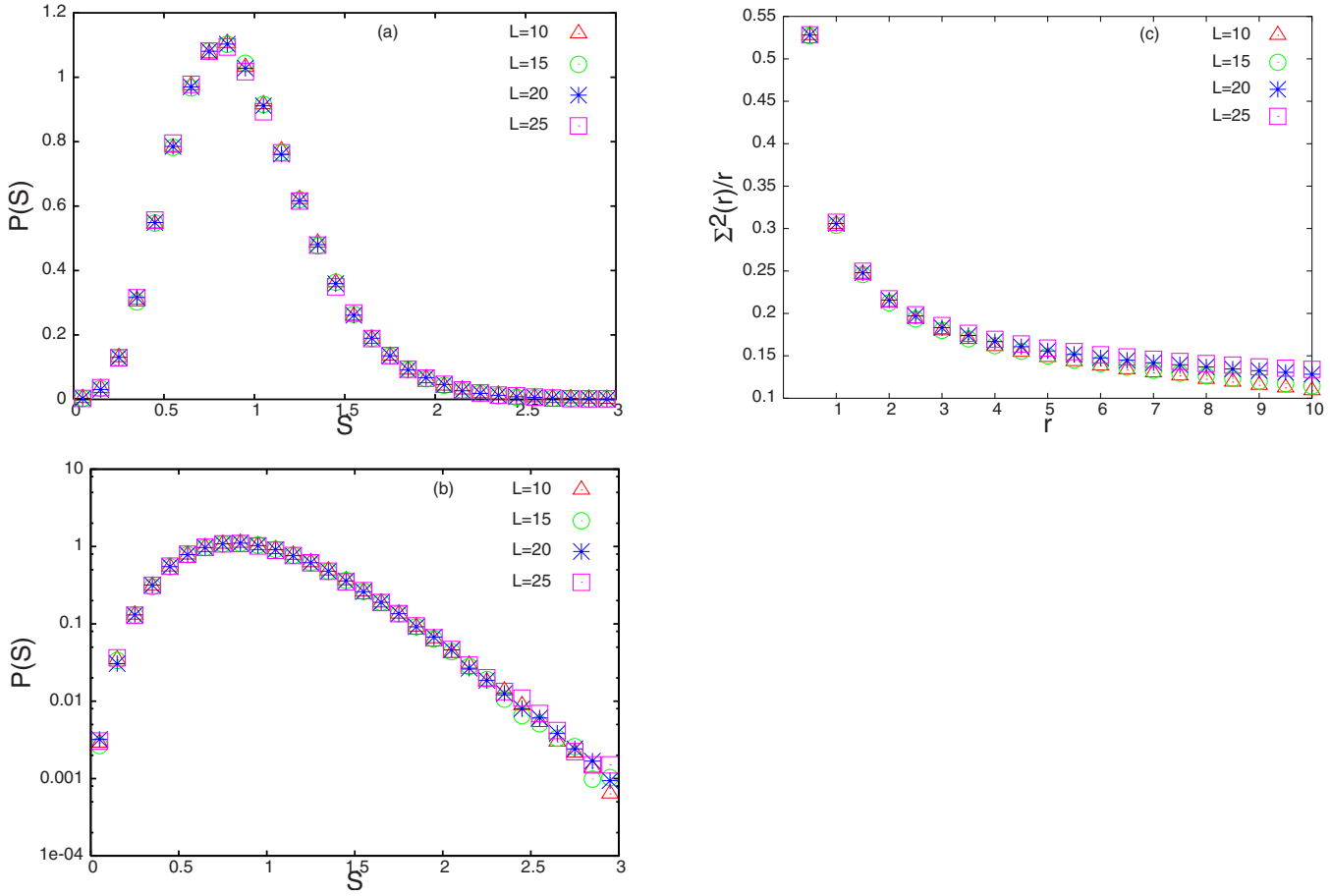

FIG. 2. (Color online) Verification of critical spectral statistics for the Anderson ensemble: (a) and (b) Linear and semilog plots for the distribution $P(S)$ of the nearest-neighbor spacing S of the eigenvalues for four system sizes; (c) number variance $\Sigma_2(r)$ for various N values. The behavior of both measures remains almost unchanged for different $N=L^2$ values, thus suggesting a critical point of spectral statistics at the chosen disorder. Here the ensemble for each N case is chosen such that we have almost 2×10^5 eigenvalues (taken from an energy range $\Delta E=20\%$ around the band center) for the statistical analysis.

$$\Lambda_{e,a}(E,Y) = |\alpha - \alpha_0| F^2 \zeta^{2d} L^{-d} (4\gamma)^{-1}, \tag{37}$$

$$\Lambda_{e,b}(E,Y) = [4(1+\mu) D_{\text{local}}^2]^{-1} \tag{38}$$

with $\alpha-\alpha_0=3$ and subscript "a" referring to AE. Here we have used the relation $D_{\text{local}}=D(L/\zeta)^d=(\zeta^d F)^{-1}$ with D as the global mean-level density, $F(E)$ as a function of energy only, $F(E)=(ND)^{-1}$, and ζ as the average localization length which is related to the typical inverse participation ratio $I_2^{\text{typ}}=\exp\langle \ln I_2\rangle \propto \zeta^{-1}$.

(ii) *Brownian ensemble.* To compare with AE [Eq. (4)], we need to consider a specific class of BEs which appears during a transition from Poisson→GSE, caused by a perturbation of the former by the latter (that is, taking H_0 and V as Poisson and GSE, respectively). This is because, similar to the Anderson transition for SOC cases, Poisson→GSE transition also occurs in the symplectic matrix space, resulting in a change of localized eigenstates to delocalized ones. The specific class of BEs can be described by an $N\times N$ ensemble of real-quaternion matrices H represented by Eq. (5) with mean and variances of the elements given by Eq. (15) and Y given by Eq. (16).

The parameter Λ_e for this case can now be given as with subscript "b" referring to the BE case with Y_0 given by Eq. (13). Note here that the initial state H_0 is chosen to be the same as for the AE case, however, it corresponds to a different physical limit, namely, $\mu\to\infty$ [which is different from the insulator limit of H given by Eq. (1)]. Approximating $D_{\text{local}}\approx D=(NF)^{-1}$ (which corresponds to the approximation $\zeta^d\simeq N$), Eq. (38) suggests the possible existence of a critical point for BEs if condition $\mu=cN^2$ is satisfied; our numerical analysis given below confirms the suggestion.

Our aim is to show that the behavior of the fluctuation measures of AE is analogous to BE at system parameters which lead to the same Λ_{measure} for both cases. The latter can be used as a condition, to obtain the parameter c for the BE analog of a given AE (note, as mentioned above, the analog for different measures may be different). As indicated by Eqs. (37) and (38), this requires a prior information about F and I_2^{typ}. Figure 1 shows the ensemble averaged F for AE and BE cases; the close agreement of curves for two sizes confirms the size independence of F for each case. Our numerical study for various sizes of two systems shows that $I_{2,a}^{\text{typ}}$

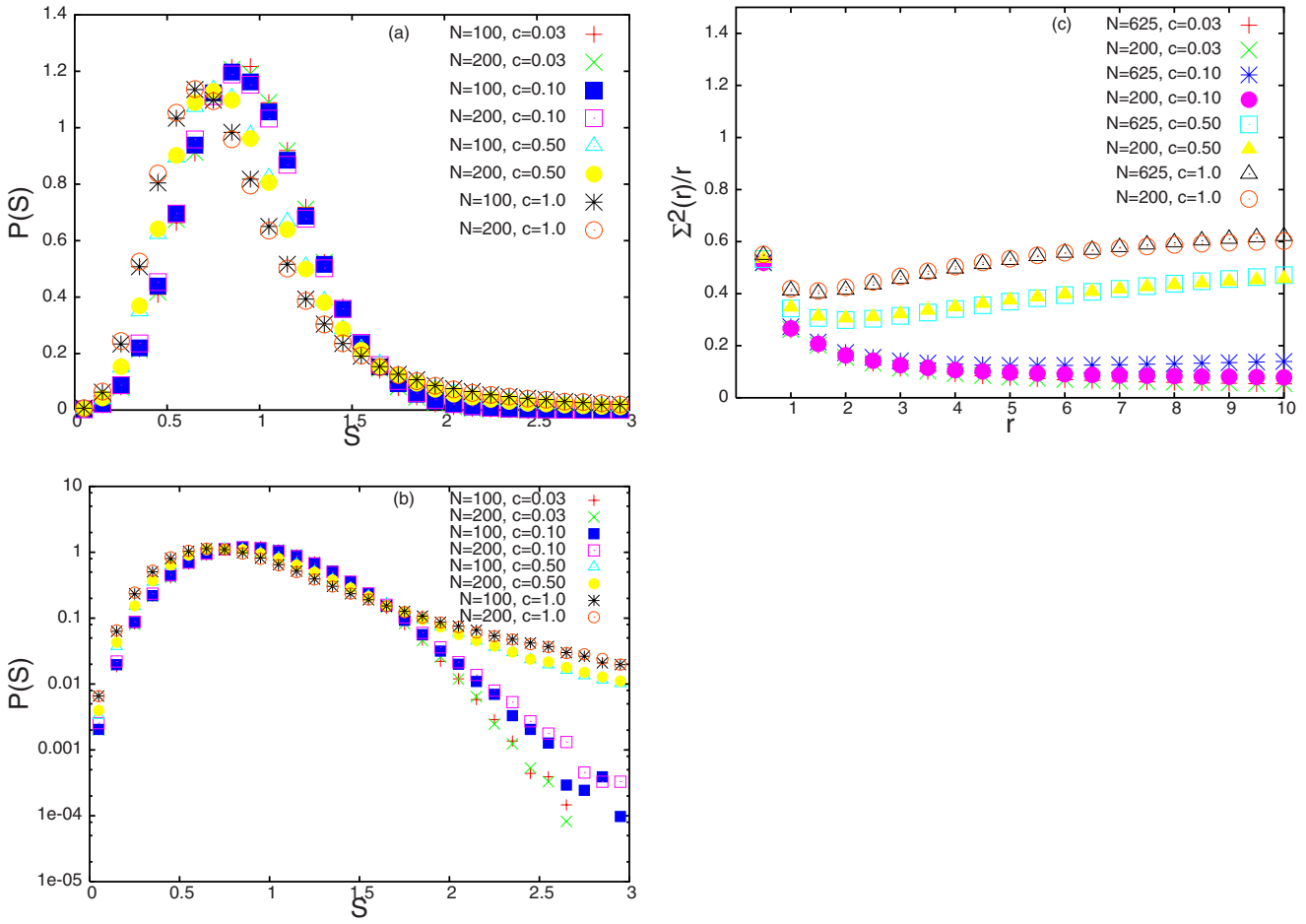

FIG. 3. (Color online) Verification of critical spectral statistics for the Brownian ensemble: (a) and (b) Linear and semilog plots for the distribution $P(S)$ of the nearest-neighbor spacing S of the eigenvalues for BEs for various c and two values of N; (c) number variance $\Sigma_2(r)$ for BEs. For a given c, the behavior of both measures remains unchanged for different N values, thus indicating a critical point of the BEs. The sample size for the statistical analysis is the same as in Fig. 2.

$\approx N^{-0.5}$ and $I_{2,b}^{\text{typ}} \propto cN^{-0.25}$. The information about I_2^{typ} and F can now be used to obtain the parameter c for BE analogs of the AE.

As Λ for the two cases is energy dependent, the fluctuation measures should be compared at precisely a given value of energy. For numerical analysis, however, one needs to consider averages over an energy range ΔE which should be sufficiently large in order to improve the statistics. On the other hand, the choice of a very large ΔE will lead to mixing of different statistics (in a range $\Delta\Lambda \propto \delta E$). This, an optimized range of ΔE, should be considered; we choose ΔE to be about 10% of the bandwidth, around the band center. For the cases considered here, the chosen ΔE corresponds to approximately 1% variation of the density of states, thus avoiding mixing of different statistics.

Equations (37) and (38) along with the I_2 and F study indicate N independence of $\Lambda_{e,a}, \Lambda_{e,b}$. As per theoretical prediction, both systems are expected to show critical behavior of the spectral statistics. To check this, we analyze large Anderson and Brownian ensembles, consisting of several thousand matrices, for various matrix sizes. Prior to the analysis, the eigenvalues are unfolded by local mean-level density. Figure 2 shows results for two spectral measures, namely, the nearest-neighbor spacing distribution $P(s)$, a measure of the short-range spectral correlations, and the number variance, a measure of long-range correlations (see [9] for their definitions) for the AE case; agreement of the curves shown in the figures for various sizes confirms size independence of the spectral fluctuations, thus confirming their critical nature for chosen disorder. Similarly, correspondence of the statistics for various sizes for the BE case with $\mu = cN^2$, shown in Fig. 3, confirms its critical nature. Note, following Eq. (38), the critical behavior of the BE with $\mu = cN^2$ requires $D_{\text{local}} \propto N^{-1}$; for BEs therefore, the relation $D_{\text{local}} = DN/\zeta^d = I_2^{\text{typ}}/F$ (giving $D_{\text{local}} \propto N^{-0.25}$ following our I_2^{typ} result) does not seem to be applicable.

To verify analogy of the spectral statistics for the same Λ_e values of AE and BE cases, we analyze the ensembles of 5000 matrices with matrix size $N=100$ for each case. Figure 4 shows the AE-BE comparison of $P(s)$; here the c parameter for the BE analog has been obtained by using $\Lambda_{e,a} = \Lambda_{e,b}$ [given by Eqs. (37) and (38)]. The good agreement between two curves verifies the analytical prediction about the single parametric dependence of the spectral correlations. This is reconfirmed by Fig. 5 showing the comparison of the number variance. Note, as predicted by our theoretical analysis, the

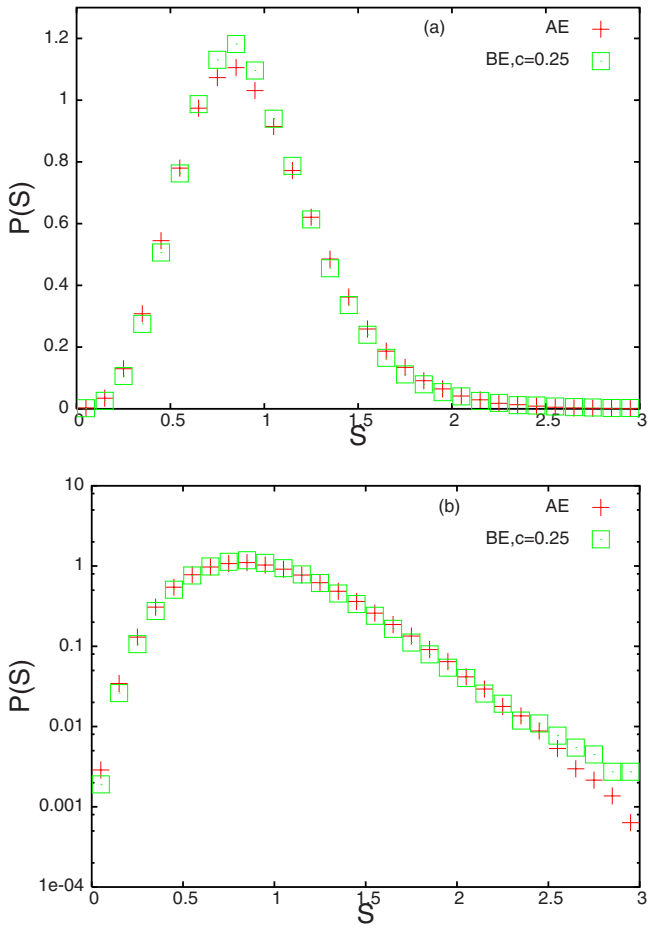

FIG. 4. (Color online) Comparison of nearest-neighbor spacing distribution $P(s)$ for AE ($\Lambda_{e,a}\approx 0.53$) and its BE analog ($c=0.25$ which gives $\Lambda_{e,b}\approx 0.41$): (a) linear plot, (b) semilog plot. The statistics is improved here by taking the energy average (in an energy range $\Delta E\simeq 40\%$ around the band center) as well as an ensemble average (an ensemble of 5×10^3 matrices, each of size $N=100$) which gives us 2×10^5 eigenvalues for the analysis. Note the relation $\Lambda_{e,a}=\Lambda_{e,b}$ suggests the BE analog to be $c=F_b^2(4\Lambda_{e,a})^{-1}=0.20$; the slight deviation of numerical analog from analytical prediction seems to be due to numerical errors.

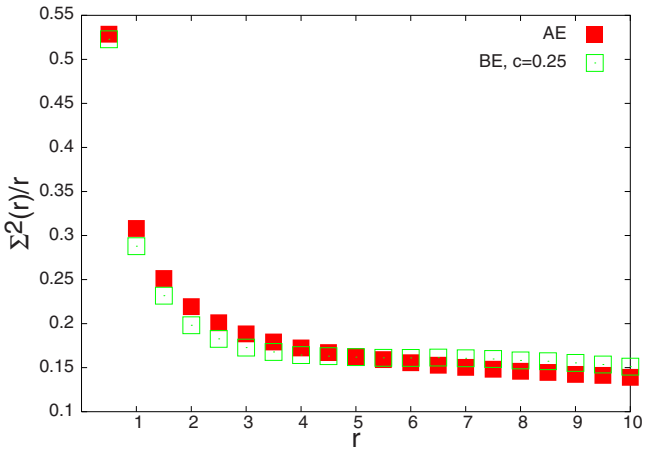

FIG. 5. (Color online) Comparison of number variance for AE (same sample size as in Fig. 4) with its BE analog ($c=0.25$). Here the chosen ΔE range is reduced as the calculation of $\Sigma_2(r)$ for large r is more sensitive [as compared to $P(S)$] to the unavoidable error introduced by considering eigenvalues in a finite energy range (due to E dependence of Λ, the statistics in principal should be compared at a given E value, however, one needs to consider the range to improve the sample size for the statistics). Note the BE analog of AE in this case is the same as in Fig. 4 but different from Figs. 6 and 7.

BE analogs for both spectral measures of AE are the same.

As discussed above, the eigenfunction fluctuations are influenced by both Λ as well as system size N. To compare Λ_{measure} dependence of an eigenfunction fluctuation measure, therefore, the same size should be taken for each system. As examples, here we consider distributions of two measures, namely, local eigenfunction intensity $P_u(u)$ and inverse participation ratio $P_I(I_2)$ (see [17] for the definition of these measures). As $Y-Y_0\propto N^{-r}$ with $r=1,2$ for AE and BE, respectively, the rescaled complexity parameter Λ_u for P_u can be approximated as $\Lambda_u=\Lambda_e/\mu\approx 2(Y-Y_0)^2/D_{\text{local}}^2$ (as $\mu\approx[2(Y-Y_0)]^{-1}$ for AE and BE cases considered here). The BE analog for the local intensity distribution of AE can then be obtained by the condition $\Lambda_{e,a}D_{\text{local},a}=\Lambda_{e,b}D_{\text{local},b}$; this gives $c=0.025$ for BE analog (using $D_{\text{local},a}=DN/\zeta^d$ and $D_{\text{local},b}=D$). However, as shown in Fig. 6 for the distribution $P_u(u')$ $[u'=(\ln u-\langle\ln u\rangle)/\langle\ln^2 u\rangle]$, our numerical analysis predicts BE with ($c=0.03$) as the analog; the small deviation from theoretical prediction again seems to be due to numerical errors.

The parameter c for the BE analog of the inverse participation ratio of AE can similarly be obtained by the relation $\Lambda_{ip,a}=\Lambda_{ip,b}$ or $\chi_a\Lambda_{e,a}=\chi_b\Lambda_{e,b}$. However, using $\chi\simeq\mu/\zeta^d$ for both AE and BE (as suggested by analysis in [17]) leads to a c value different from the one obtained by numerical analysis, namely, $c=0.4$ [see Fig. 7 showing $P_I(\ln I_2)$ behavior]. The error seems to originate from the approximation used for χ. Further studies of AEs with different system condition and a numerical search for their BE analogs can be helpful to explore a correct behavior of χ; we hope to pursue this analysis in the near future.

VI. CONCLUSION

In the end we summarize our main results.

The Hermitian operators governing the dynamics of a large class of complex systems with half-integer spin may depend on many system parameters, however, their statistical fluctuations seem to be governed by a single parameter Λ. This indicates a possible characterization of complex systems by their complexity parameters. The result is analogous to systems with integer spin and with or without time-reversal symmetry. The surprising result suggests that the sample-to-sample fluctuations of physical properties are not sensitive to the origin of the interactions, random or nonrandom, and are influenced only by the degree of uncertainty associated with their determination. This suggests a deep rooted universality as well as a web of connection hidden underneath the statistical behavior of complex systems which should be investigated in detail.

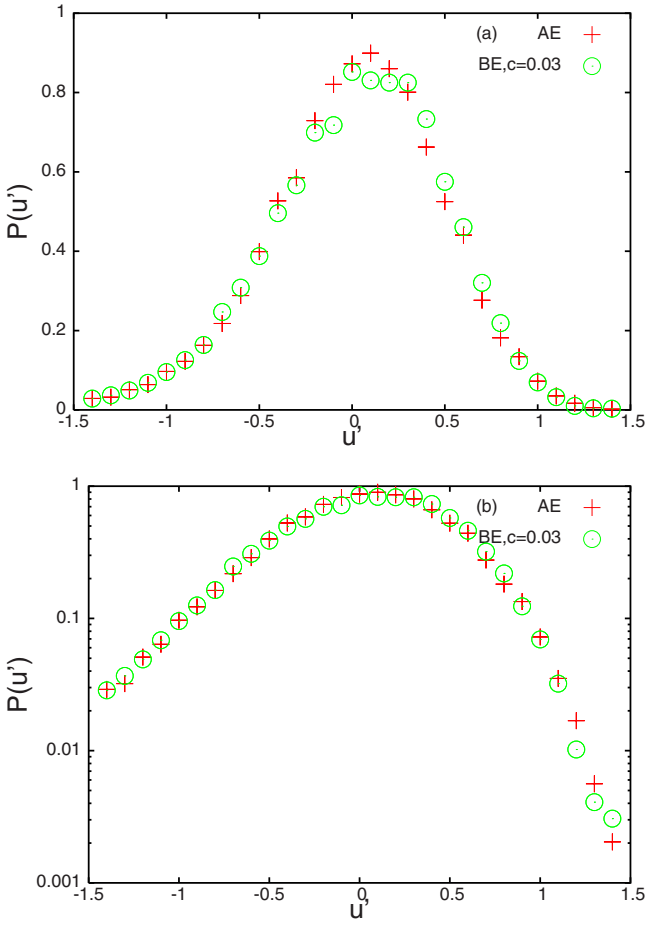

FIG. 6. (Color online) Comparison of eigenfunction statistics for AE and BE: Distribution $P_u(u')$ with $u'=(\ln u-\langle u\rangle)/\langle \ln^2 u\rangle$ of the local intensity of an eigenfunction near band center for AE and its BE analog ($c=0.03$). The parts (a) and (b) of the figure correspond to linear and semilog plot, respectively. The statistics is improved here by taking the average over eigenfunctions in an energy range ΔE around the band center as well as the average over an ensemble of 5×10^3 matrices, each of size $N=100$. Here, the BE analog is obtained first by finding c by the relation $t_a=t_b$, where $t_s \equiv \Lambda_{e,s} D_{\text{local},s}$ and subsequent numerical analysis of BEs in the neighborhood of theoretical c; the latter gives $c=0.03$ ($t_b\approx 0.047$) to be closest to the AE curve. Note $t_a\approx 0.057$ for the AE case which implies its BE analog to be $c=(4\sqrt{\pi N t_a})^{-1}=0.025$.

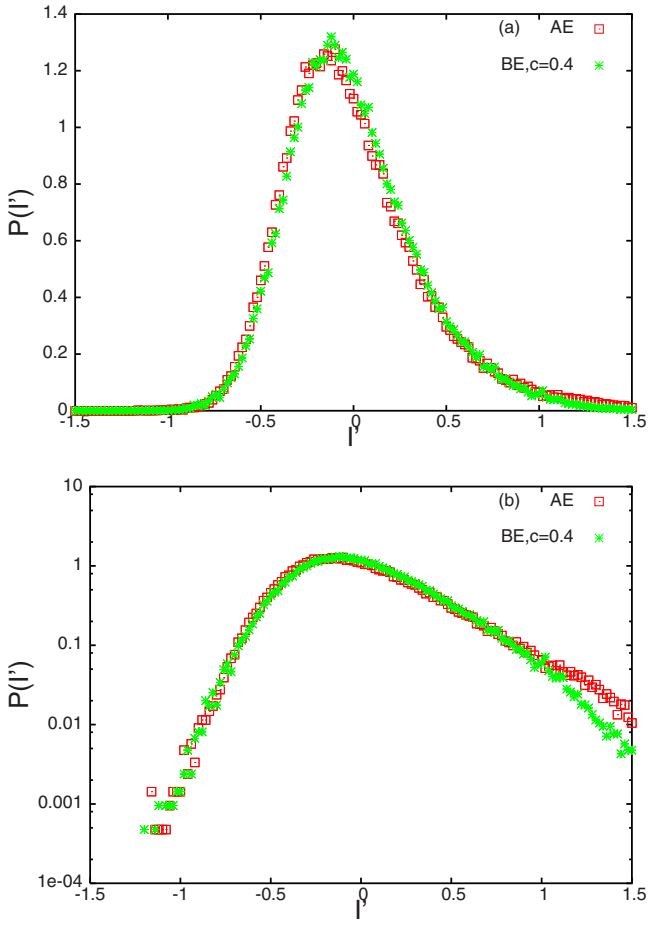

FIG. 7. (Color online) Distribution $P(I_2')$ of the rescaled inverse participation ratio $I_2'=\ln(I_2/I_2^{\text{typ}})$ for AE and its BE analog: (a) linear plot, (b) tail behavior (semilog plot). Here the sample size is the same as in Fig. 6. Note the analog is different from Figs. 4–6. Our numerical analysis shows $c=0.2$, quite close too, which suggests $\chi\simeq 1$.

ACKNOWLEDGMENT

The authors are grateful to Professor M. Berry for useful suggestions which helped improve this work.

APPENDIX A: PROOF OF EQS. (20)–(22)

The use of the eigenvalue equation $HS=S\Lambda$, with S as a symplectic matrix and Λ the eigenvalue matrix, leads to the following:

$$\sum_j H_{ij}S_{jn}=\lambda_n S_{in}. \tag{A1}$$

Differentiating the above equation with respect to $H_{kl;s}$, then multiplying both sides by S^R_{ni}, followed by a summation over all i's, leads to

$$\frac{\partial \lambda_n}{\partial H_{kl;s}}=\sum_{i,j} S^R_{ni}\frac{\partial H_{ij}}{\partial H_{kl;s}}S_{jn}, \tag{A2}$$

where we have used the eigenfunction orthonormalization condition $\Sigma_i S^R_{ni}S_{im}=\delta_{nm}$. Now using $H_{kl}\equiv\Sigma_{s=1}^4 H_{kl;s}\tau_s$, along with constraint $H_{kl;s}=(-1)^{s-1}H_{lk;s}$ in Eq. (A2) leads to Eq. (20).

Equation (21) can similarly be proved. Multiplying both sides of Eq. (A1) by S^R_{mi} $(m\neq n)$ followed by a summation over all i's, we obtain

$$\sum_j S^R_{mj}\frac{\partial S_{jn}}{\partial H_{kl;s}}=\frac{1}{\lambda_n-\lambda_m}\sum_{i,j} S^R_{mi}\frac{\partial H_{ij}}{\partial H_{kl;s}}S_{jn}. \tag{A3}$$

A multiplication of both sides by S_{rm} followed by a summation over all m's then gives Eq. (21).

Equation (22) can be proved following similar steps, however, one should now begin with $\Sigma_i S^R_{ni}H_{ij}=\lambda_n S^R_{nj}$.

APPENDIX B: DETAILED PROOFS OF EQS. (23)–(25)

Proof of Eq. (23). As $\lambda_n=\Sigma_{ij}S^R_{ni}H_{ij}S_{jn}$ and $H_{kl;s}=a_sH_{lk;s}$ with $a_1=1$, $a_2=a_3=a_4=-1$, we obtain [with the help of Eq. (20)]

$$\sum_{s=1}^{3}\sum_{k\le l}\frac{\partial\lambda_n}{\partial H_{kl;s}}H_{kl;s}=\sum_{k\le l}\frac{1}{g_{kl}}[S^R_{nk}(\sum_s \tau_sH_{kl;s})S_{ln} + S^R_{nl}(\sum_s a_s\tau_sH_{kl;s})S_{kn}] = \frac{1}{2}\sum_{k,l}(S^R_{nk}H_{kl}S_{ln}+S^R_{nl}H_{lk}S_{kn})=\lambda_n. \tag{B1}$$

Here the last step is obtained by using the relation $\Sigma_{k\le l}f_{kl}/g_{kl}=(1/2)\Sigma_{k,l}f_{kl}$.

Proof of Eq. (24). We have

$$\begin{aligned}F_1 &\equiv \sum_{k\le l}g_{kl}\sum_{s=1}^{4}\frac{\partial\lambda_n}{\partial H_{kl;s}}\frac{\partial\lambda_m}{\partial H_{kl;s}}\\ &=\sum_{s=1}^{4}\sum_{k,l}(S^R_{nk}\tau_sS_{ln}S^R_{mk}\tau_sS_{lm}+a_sS^R_{nl}\tau_sS_{kn}S^R_{mk}\tau_sS_{lm})\\ &=\sum_{k,l}S^R_{nk}(\sum_s\tau_sS_{ln}S^R_{mk}\tau_s)S_{lm}\\ &\quad+\sum_s\sum_l a_sS^R_{nl}\tau_s(\sum_k S_{kn}S^R_{mk})\tau_sS_{lm},\end{aligned} \tag{B2}$$

where Eq. (B2) has been obtained by using $a_s^2=1$ (for all s) and Eq. (20). Now as

$$\sum_{s=1}^{4}\tau_sS_{ln}S^R_{mk}\tau_s=-S_{km}S^R_{nl}\sum_{s=1}^{4}a_s \tag{B3}$$

and $\Sigma_kS^R_{mk}S_{kn}=\delta_{mn}$, $\tau_s^2=a_s$, $\Sigma_sa_s=-2$, and $\Sigma_sa_s^2=4$, Eq. (B2) can be rewritten as

$$\begin{aligned}F_1&=-\sum_{k,l}S^R_{nk}S_{km}S^R_{nl}S_{lm}+\delta_{nm}\sum_s\sum_l a_sS^R_{nl}\tau_s^2S_{lm}\\ &=\delta_{nm}(-2+\sum_s a_s^2)=2\delta_{nm}.\end{aligned} \tag{B4}$$

Proof of Eq. (25). We have

$$\sum_{k\le l}g_{kl}\sum_{s=1}^{4}\frac{\partial^2\lambda_n}{\partial H^2_{kl;s}}=\sum_{k\le l;s}\left(\frac{\partial S^R_{nk}}{\partial H_{kl;s}}\tau_sS_{ln}+S^R_{nk}\tau_s\frac{\partial S_{ln}}{\partial H_{kl;s}} + a_s\frac{\partial S^R_{nl}}{\partial H_{kl;s}}\tau_sS_{kn}+a_sS^R_{nl}\tau_s\frac{\partial S_{kn}}{\partial H_{kl;s}}\right). \tag{B5}$$

Now using Eqs. (21) and (22), we obtain

$$\begin{aligned}\sum_{k\le l}g_{kl}\sum_{s=1}^{4}\frac{\partial^2\lambda_n}{\partial H^2_{kl;s}}&=\sum_m\frac{2}{\lambda_n-\lambda_m}\sum_{s=1}^{3}\sum_{k,l}(a_sS^R_{nl}\tau_sS_{km}S^R_{mk}\tau_sS_{ln} + S^R_{nk}\tau_sS_{lm}S^R_{mk}\tau_sS_{ln})\\ &=\sum_{m\ne n}\frac{2}{\lambda_n-\lambda_m}\left[\sum_l\sum_s a_sS^R_{nl}\tau_s(\sum_k S_{km}S^R_{mk})\times\tau_sS_{ln}+\sum_{k,l}S^R_{nk}(\sum_s\tau_sS_{lm}S^R_{mk}\tau_s)S_{ln}\right]\\ &=\sum_{m\ne n}\frac{2}{\lambda_n-\lambda_m}\left(\sum_s a_s^2\sum_l S^R_{nl}S_{ln} - \sum_{k,l}S^R_{nk}S_{km}S^R_{ml}S_{ln}\right)\\ &=\sum_{m\ne n}\frac{2}{\lambda_n-\lambda_m}\left(\sum_s a_s^2-\delta_{nm}\right)\\ &=\sum_{m\ne n}\frac{8}{\lambda_n-\lambda_m}.\end{aligned} \tag{B6}$$

[1] I. Zutic, J. Fabian, and S. Das Sarma, Rev. Mod. Phys. **76**, 323 (2004).
[2] D. D. Awschalom, D. Loss, and N. Samarth, *Semiconductor Spintronics and Quantum Computation*, 1st ed. (Springer, New York, 2002).
[3] P. Zahn, in *Materials for Tomorrow Theory, Experiments and Modelling*, edited by S. Gemming, M. Schreiber, and J.-B. Suck (Springer, Berlin, 2007).
[4] M. Tanaka and T. S. Jones, J. Cryst. Growth **278**, 25 (2005).
[5] Many new applications of spintronics and several other references can be found, e.g., http://www.spintronics-info.com, as well as cond-mat archives.
[6] M. Znidaric, Tomaz Prosen, and Peter Prelovsek, e-print arXiv:0706.2539.
[7] Y. Alhassid, Rev. Mod. Phys. **72**, 895 (2000).
[8] P. Shukla, Phys. Rev. E **62**, 2098 (2000).
[9] F. Haake, *Quantum Signatures of Chaos* (Springer, Berlin, 1991); M. L. Mehta, *Random Matrices* (Academic, New York, 1991); C. E. Porter, *Statistical Theory of Spectra: Fluctuations* (Academic, New York, 1965).
[10] T. Guhr, G. A. Muller-Groeling, and H. A. Weidenmuller, Phys. Rep. **299**, 189 (1998).
[11] T. A. Brody, J. Flores, J. B. French, P. A. Mello, A. Pandey, and S. S. M. Wong, Rev. Mod. Phys. **53**, 385 (1981).
[12] S. N. Evangelou and D. E. Katsanos, J. Stat. Phys. **85**, 525 (1996).
[13] R. Scharf, J. Phys. A **22**, 4223 (1989).
[14] R. Balian, Nuovo Cimento B **57B**, 183 (1968).
[15] M. V. Berry (private communication).
[16] P. Shukla, Phys. Rev. E **71**, 026226 (2005).
[17] P. Shukla, Phys. Rev. E **75**, 051113 (2007).
[18] F. Dyson, J. Math. Phys. **3**, 1191 (1962).
[19] A. Pandey, Chaos, Solitons Fractals **5**, 1275 (1995).
[20] P. Shukla, J. Phys.: Condens. Matter **17**, 1653 (2005).